Talanta 82 (2010) 1193–1199

Contents lists available at ScienceDirect

Talanta

journal homepage: www.elsevier.com/locate/talanta

Electrocatalytic oxidation behavior of guanosine at graphene, chitosan and Fe_3O_4 nanoparticles modified glassy carbon electrode and its determination

Huanshun Yin[a,b], Yunlei Zhou[c], Qiang Ma[a], Shiyun Ai[a,*], Quanpeng Chen[b], Lusheng Zhu[b]

[a] College of Chemistry and Material Science, Shandong Agricultural University, Taian 271018, Shandong, China
[b] College of Resources and Environment, Shandong Agricultural University, Taian 271018, Shandong, China
[c] College of Life Science, Beijing Normal University, Beijing 100875, China

ARTICLE INFO

Article history:
Received 8 March 2010
Received in revised form 19 June 2010
Accepted 24 June 2010
Available online 3 July 2010

Keywords:
Graphene
Guanosine
Chitosan
Fe_3O_4 nanoparticles
Electrochemical determination

ABSTRACT

A graphene, chitosan and Fe_3O_4 nanoparticles (nano-Fe_3O_4) modified glassy carbon electrode (graphene–chitosan/nano-Fe_3O_4/GCE) was fabricated. The modified electrode was characterized by scanning electron microscope and electrochemical impedance spectroscopy. The electrochemical oxidation behavior of guanosine was investigated in pH 7.0 phosphate buffer solution by cyclic voltammetry and differential pulse voltammetry. The experimental results indicated that the modified electrode exhibited an electrocatalytic and adsorptive activities towards the oxidation of guanosine. The transfer electron number (n), transfer proton number (m) and electrochemically effective surface area (A) were calculated. Under the optimized conditions, the oxidation peak current was proportional to guanosine concentration in the range of 2.0×10^{-6} to 3.5×10^{-4} mol L^{-1} with the correlation coefficient of 0.9939 and the detection limit of 7.5×10^{-7} mol L^{-1} (S/N = 3). Moreover, the modified electrode showed good ability to discriminate the electrochemical oxidation response of guanosine, guanine and adenosine. The proposed method was further applied to determine guanosine in spiked urine samples and traditional Chinese medicines with satisfactory results.

1. Introduction

Guanosine is the important intermediate in food industry and pharmaceutical industry, which can be used to synthesize the food freshener and antiviral drug. Guanosine is also a naturally endogenous compound with a wide spectrum of biological activities. It can present neuroprotective effects in cultured neurons submitted to hypoxia and increase glutamate uptake in cultured astrocytes [1]. Moreover, guanosine can also exert trophic effects on neural cells [2], protect brain slices submitted to hypoxia/hypoglycemia [1], stimulate the removal of extracellular glutamate by astrocytes [3], culture medium from astrocytes treated with guanosine prevented NMDA-induced toxicity in neurons [4] and treat disease, including epilepsy and anxiety [5]. And what is more, the changes of guanosine concentration in body fluids have been used to indicate the presence of various diseases. For instance, the levels of guanosine in urine and plasma have been testified to be related to carcinoma [6] and liver disease [7], respectively. Therefore, it is necessary to establish a sensitive and reliable method for guanosine detection and determination.

Electrochemical technique is a powerful method for the detection of guanosine due to the advantages of rapid response, low cost, simple operation, time saving, high sensitivity and excellent selectivity. For instance, Goyal et al. [7] used fullerene–C_{60}-modified glassy carbon electrode (GCE) to simultaneously determine guanosine and adenosine. Compared with the bare GCE, the modified electrode exhibited an apparent shift of the oxidation potentials in the cathodic direction and a significantly enhancement in the oxidation peak current for both the biomolecules. Sun et al. investigated the electrochemical behavior of guanosine on multi-walled carbon nanotubes (MWCNTs) and ionic liquid 1-ethyl-3-methylimidazolium tetrafluoroborate ($EMIMBF_4$) modified CPE [8]. The fabricated electrode showed obviously electrocatalytic activity towards the oxidation of guanosine, and the detection limit was 7.8×10^{-8} mol L^{-1}. Due to the advantages of low background current and wide potential window in aqueous media, boron doped diamond electrode (BDD electrode) was also applied to investigated the electrochemical behavior of guanosine by Fortin et al. [9]. Though some satisfactory results have been obtained using electrochemical technique, it is still interesting to investigate novel electrode modified material for guanosine determination.

In recent years, a new kind of carbon material, graphene, has attracted more and more attentions both from the fundamen-

* Corresponding authors. Tel.: +86 538 8247660; fax: +86 538 8242251.
E-mail addresses: ashy@sdau.edu.cn, chemashy@yahoo.com.cn (S. Ai), lushzhu@sdau.edu.cn (L. Zhu).

0039-9140/$ – see front matter © 2010 Elsevier B.V. All rights reserved.
doi:10.1016/j.talanta.2010.06.030

tal studies and practical aspects due to its specifical properties, such as excellent electrical conductivity, high surface area, good mechanical strength, high thermal conductivity and high mobility of charge carriers. Many researchers have investigated the feasibility of graphene in electroanalytical chemistry as a novel electrode modified material. For instance, Mao and co-workers [10] prepared graphene film electrode with tunable dimension with vaseline as the insulating binder, and this new kind of carbon-based film electrode with tailor-made dimensions showed a good electrochemical activity as well as high stability which was demonstrated in $Fe(CN)^{3-/4-}$ solution. Li's group has demonstrated that graphene-based electrochemical sensors was an effective tool for determination of dopamine and ethanol [11,12]. Niu's group constructed two kinds of graphene-based electrochemical glucose biosensors, and the results suggested that graphene exhibited potential application in biosensor [13,14], and the similar results were also obtained by other researchers [15–18]. Moreover, graphene also showed excellent electrocatalytic activity towards H_2O_2 [19–21], β-nicotinamide adenine dinucleotide (NADH) [20–22], hydrazine [23], tripropylamine [24] and DNA [21]. Therefore, graphene-based sensors should be an appropriate platform for electrochemical sensing and biosensing. In addition, Fe_3O_4 magnetic nanoparticles (nano-Fe_3O_4) have also attracted an increasing interest in biotechnology and medicine [25]. Due to their good biocompatibility, strong superparamagnetic property, low toxicity, easy preparation and high adsorption ability, nano-Fe_3O_4 has been widely investigated as electrode modified material in sensors and biosensors [26,27]. However, to the best of our knowledge, the determination of guanosine using graphene and Fe_3O_4 nanoparticles modified electrode has not yet been investigated.

In this work, we fabricated a novel electrochemical sensor based on a glassy carbon electrode (GCE) modified with graphene and Fe_3O_4 magnetic nanoparticles. The electrochemical oxidation behavior of guanosine was investigated. The fabricated electrode showed excellent electrocatalytic activity towards guanosine oxidation with the increased oxidation peak current and the decreased oxidation peak potential. For further confirmation of the feasibility of practical application, the guanosine contents in real urine samples traditional Chinese medicines were determined.

2. Experiments

2.1. Reagents and apparatus

Guanosine (GS), guanine (G) and adenosine (AS) were purchased from Sigma. Graphite powder (spectroscopically pure reagent) was obtained from Qingdao Hensen Graphite Co. Ltd. (China). Chitosan was from Aldrich (USA). Graphene and nano-Fe_3O_4 were synthesized according to Refs. [28–30]. Guanosine, adenosine and guanine stock solutions were prepared with 0.1 M NaOH and kept in darkness at 4 °C. Working solutions were freshly prepared before use by diluting the stock solution. Phosphate buffer solution (PBS, 0.1 mol L^{-1}) was prepared by mixing the stock solution of 0.1 mol L^{-1} NaH_2PO_4 and 0.1 mol L^{-1} Na_2HPO_4. A 0.5 wt.% chitosan solution was prepared by dissolving chitosan in 1 wt.% acetic acid solution with magnetic stirring for about 1 h, then the pH of the solution was adjusted to pH 5.0 with a concentrated NaOH solution. Other chemicals were analytical reagent grade and all solutions were prepared with double distilled deionized water from quartz. All the reagents were used without further purification.

Electrochemical experiments were performed with a CHI660C electrochemical workstation (Shanghai Chenhua Co., China) with a conventional three-electrode cell. A bare or modified glassy carbon electrode (CHI104, d = 3 mm, Shanghai Chenhua Co., China) was used as working electrode. A saturated calomel electrode (SCE) and a platinum wire were used as reference and auxiliary electrodes, respectively. The transmission electron microscope (TEM) images were obtained at JEOL-1200 EX TEM (Japan). All the measurements were carried out at room temperature (25 ± 0.5 °C).

2.2. Preparation of graphene–chitosan/nano-Fe_3O_4/GCE

Before modification, the bare GCE was polished to obtain a mirror-like surface with 0.3 μm alumina slurry, then washed successively with anhydrous alcohol and water in an ultrasonic bath for 3 min and dried in N_2 blowing. 1.5 mg graphene was added into 1 mL 0.5% chitosan solution, followed by ultrasonication for 2 h to form a homogenous mixture of graphene–chitosan. 2.5 mg nano-Fe_3O_4 was added into 1 mL water and sonicated for 2 h to obtain a homogeneously dispersed solution. 5 μL of nano-Fe_3O_4 dispersion was deposited on the fresh prepared GCE surface. After solvent evaporation, the electrode surface was thoroughly rinsed with water and dried in the air. Then, 5 μL of graphene–chitosan composite was dropped on the surface of nano-Fe_3O_4/GCE. After drying under ambient condition, the graphene–chitosan/nano-Fe_3O_4/GCE was rinsed with water to remove the unimmobilized mixture. For comparison, Chitosan/GCE, nano-Fe_3O_4/GCE and graphene–chitosan/GCE were fabricated with the similar procedures.

2.3. Electrochemical measurements

Unless otherwise stated, 0.1 mol L^{-1} PBS (pH 7.0) was used as the supporting electrolyte. A certain volume of guanosine solution and 10 mL 0.1 mol L^{-1} PBS was added into an electrochemical cell and then the three-electrode system was installed on it. After a 350-s accumulation at the potential of 0.60 V, cyclic voltammograms were recorded in the potential range from 0.20 to 1.25 V with the scan rate of 100 mV s^{-1}. The differential pulse voltammetry was carried out with the parameters of increment potential, 0.004 V; pulse amplitude, 0.05 V; pulse width, 0.05 s; sample width, 0.0167 s; pulse period, 0.2 s; quiet time, 2 s.

2.4. Traditional Chinese medicine samples preparation

Three kinds of traditional Chinese medicines, *Pinellia ternate*, *Raidx astragali* and *Angelica sinensis*, were purchased from a local drugstore. The sample was first crashed to fine powder and 5.0 g was weighed accurately. Then the samples were extracted with 30 mL of double distilled deionized water for 1 h by ultrasonication. After centrifuged for 5 min and filtered, the filtrate was collected and concentrate to 5 mL.

3. Results and discussion

3.1. Characterization of chitosan dispersed graphene and nano-Fe_3O_4

Fig. 1A shows the TEM image of graphene nanosheets, clearly clarifying the crumpled and wrinkled flake-like structure. The morphology of nano-Fe_3O_4 was also investigated by TEM and shown in Fig. 1B. It can be found that particles of nano-Fe_3O_4 are spherical and the size of the spherical particles is around 20–30 nm.

3.2. Characteristics of the modified electrode

Electrochemical impedance spectroscopy was used to characterize the electron transfer properties of GCE after different surface modification. Fig. 2 shows the Nyquist plot of the bare GCE (a), nano-Fe_3O_4/GCE (b), chitosan/GCE (c), graphene–chitosan/GCE (d) and graphene–chitosan/nano-Fe_3O_4/GCE (e) in 5×10^{-3} mol L^{-1}

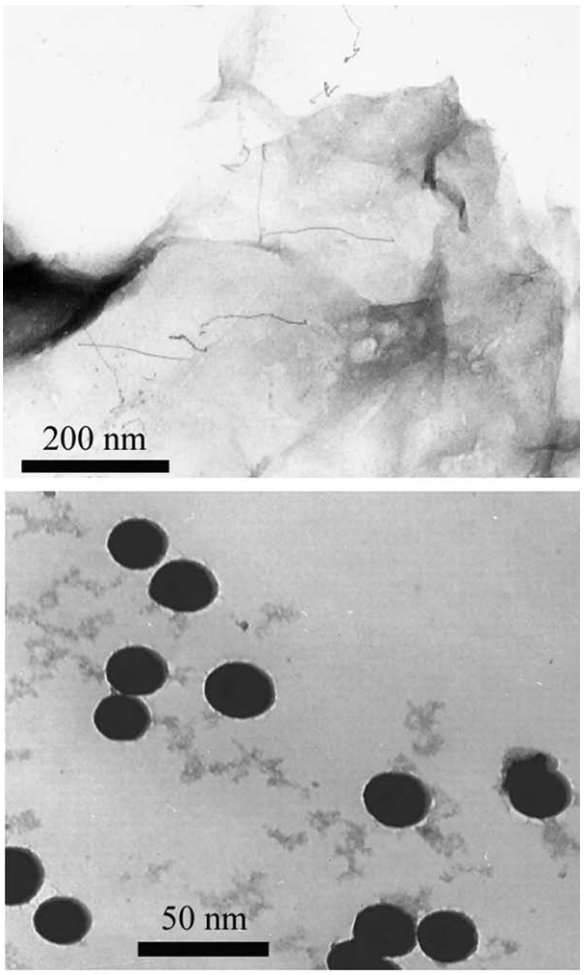

Fig. 1. TEM image of graphene nanosheet (A) and nano-Fe_3O_4 (B).

$[Fe(CN)_6]^{3-/4-}$ containing 0.1 mol L^{-1} KCl. For the bare GCE, the value of electron transfer resistance (R_{et}) was 668.8 Ω, revealing a relatively big semicircle domain. When nano-Fe_3O_4 was immobilized on the GCE surface, the R_{et} decreased to 499.3 Ω, which could be attributed to the conductivity of Fe_3O_4 nanoparticles. On the contrary, due to the non-conductivity of chitosan film, the R_{et} of the chitosan/GCE increased more significantly (3547.4 Ω), reflected by a larger semi-circle at higher frequencies

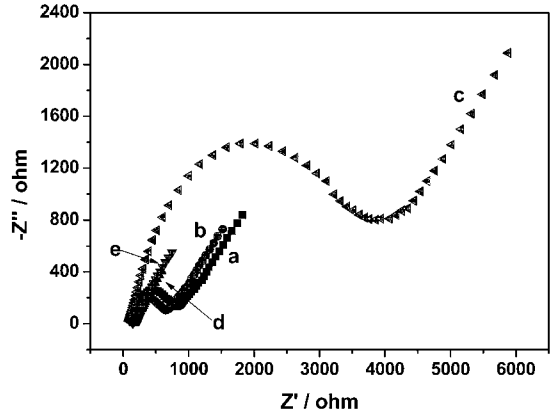

Fig. 2. Nyquist plot of the bare GCE (a), nano-Fe_3O_4/GCE (b), chitosan/GCE (c), graphene–chitosan/GCE (d) and graphene–chitosan/nano-Fe_3O_4/GCE (e). The frequency range was from 10^{-1} to 10^5 Hz.

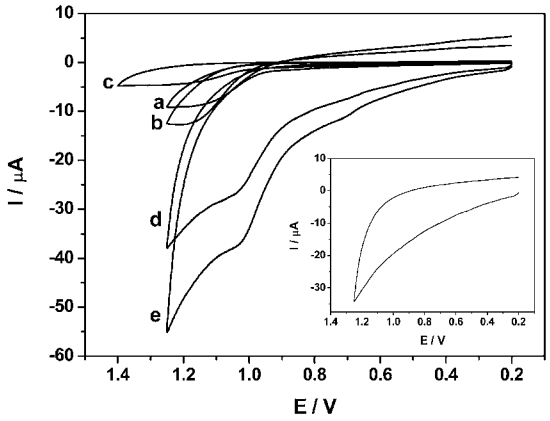

Fig. 3. Cyclic voltammograms of 2.0×10^{-4} mol L^{-1} guanosine at GCE (a), nano-Fe_3O_4/GCE (b), chitosan/GCE (c), graphene–chitosan/GCE (d) and graphene–chitosan/nano-Fe_3O_4/GCE (e) in 0.1 mol L^{-1} pH 7.0 PBS. Insert: the cyclic voltammogram of graphene–chitosan/nano-Fe_3O_4/GCE in 0.1 mol L^{-1} pH 7.0 PBS.

region. Moreover, an obvious decrease in the interfacial electron transfer resistance was observed when graphene was dispersed in chitosan film. There is no doubt that the decreased R_{et} could be ascribed to graphene, which improved the conductivity of the GCE and facilitated the electron transfer between solution and electrode interface. In addition, the R_{et} of graphene–chitosan/nano-Fe_3O_4/GCE further decreased. It might be caused by the synergetic effect of graphene–chitosan composite and nano-Fe_3O_4. This result also indicated that graphene–chitosan/nano-Fe_3O_4/GCE was successfully fabricated.

3.3. Electrochemical oxidation behavior of guanosine

The electrochemical oxidation behavior of 2.0×10^{-4} mol L^{-1} guanosine was investigated in pH 7.0 PBS by cyclic voltammetry and the results were shown in Fig. 3. No redox peak was observed at graphene–chitosan/nano-Fe_3O_4/GCE in blank PBS, indicating that the graphene–chitosan/nano-Fe_3O_4 composite is non-electroactive in the selected potential region. In 2.0×10^{-4} mol L^{-1} guanosine solution, an irreversible oxidation peak appeared at GCE with the peak potential of 1.22 V (curve a), which could be ascribed to the electrochemical oxidation of guanosine undoubtfully. On the nano-Fe_3O_4/GCE, the oxidation peak of guanosine was observed at 1.20 V and the oxidation peak current increased obviously (curve b). The increased peak current and almost unchanged peak potential indicated that nano-Fe_3O_4 can effectively adsorb guanosine onto the electrode surface, which can be attributed to that the large surface area of nano-Fe_3O_4 immobilized on the GCE surface can increase the electrochemically adsorptive site and then increase the oxidation current. However, a decreased oxidation response was observed at chitosan/GCE (1.27 V, curve c), even than GCE, which can be attributed to the non-conductivity of chitosan. On the graphene–chitosan/GCE (curve d), the oxidation peak current increased significantly accompanied the oxidation peak potential shifting more negatively (1.05 V) when compared with the bare GCE, chitosan/GCE and nano-Fe_3O_4/GCE, which could be attributed to the excellent conductivity, large surface area and good catalytic activity of graphene. Moreover, the oxidation peak current increased further and the oxidation peak potential shifted more negatively to 1.04 V when graphene–chitosan composite and nano-Fe_3O_4 was immobilized on the GCE surface (curve e). The net values of the oxidation peak current of guanosine obtained at graphene–chitosan/nano-Fe_3O_4/GCE (8.52 μA) was about 2.49, 4.95, 1.84 and 1.18 times higher than that on the bare GCE (3.41 μA), chitosan/GCE (1.72 μA), nano-Fe_3O_4/GCE (4.66 μA) and

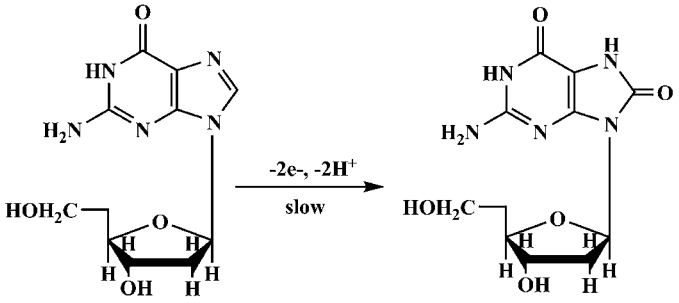

Fig. 4. The electrochemical oxidation mechanism of guanosine at graphene–chitosan/nano-Fe_3O_4/GCE.

graphene–chitosan/GCE (7.17 μA), respectively. This result indicated that the graphene–chitosan and nano-Fe_3O_4 can improve the oxidation of guanosine. Considering the sensitivity and selectivity, graphene–chitosan/nano-Fe_3O_4/GCE was chosen as the working electrode in the following investigations.

It has been reported that the electrochemical oxidation of guanosine at glassy carbon, carbon ionic liquid and pyrolytic graphite electrodes involves four-electrons and four protons by two steps [8,31]. The guanosine molecule is first electrochemically oxidized to give 8-oxyguanine via a $2e^-/2H^+$ process. Since the latter is more easily oxidized than guanosine, it is immediately further oxidized in another $2e^-/2H^+$ reaction to give an unstable intermediate, and the intermediate will further hydrolyzed to form stable diol. According to the previous reports and the results obtained in this work (see Section 3.4), the electrochemical oxidation mechanism of guanosine at graphene–chitosan/nano-Fe_3O_4/GCE can be expressed as in Fig. 4.

3.4. Optimization of determination conditions

The effect of solution pH on the electrochemical response of 1.0×10^{-4} mol L^{-1} guanosine at graphene–chitosan/nano-Fe_3O_4/GCE was investigated in the pH range from 5.7 to 8.0 by cyclic voltammetry. As can be seen in Fig. 5, the solution pH obviously influenced the oxidation peak current and the maximum current response was obtained at pH 7.0. Thus this pH was chosen for the subsequent analytical experiments. The solution pH also influenced the oxidation peak potential (E_{pa}) of guanosine and the relationship between E_{pa} and pH was also shown in Fig. 5. The regression equation can be expressed as E_{pa} (V) = −0.066 pH + 1.51 (R = 0.9939). A slope of 66 mV pH^{-1} indicated that there were the equal numbers of proton and electron involved in electrode reaction, which is in accordance with previous reports [8,32].

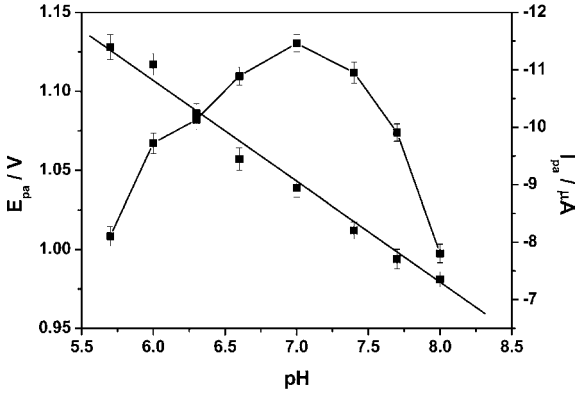

Fig. 5. Influence of pH on the oxidation peak current and potential of 1.0×10^{-4} mol L^{-1} guanosine.

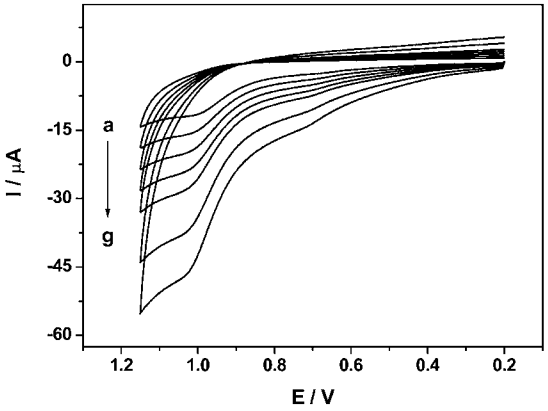

Fig. 6. The effect of scan rate on the oxidation of 1.5×10^{-4} mol L^{-1} guanosine. (a)–(g) 20, 40, 60, 80, 100, 150 and 200 mV s^{-1}.

The influence of scan rate on the electrochemical response of 1.5×10^{-4} mol L^{-1} guanosine was also investigated by cyclic voltammetry and the results were shown in Fig. 6. With increasing the scan rate from 20 to 200 mV s^{-1}, the oxidation peak current increased gradually and linearly, indicating that the guanosine oxidation at graphene–chitosan/nano-Fe_3O_4/GCE is an adsorption-controlled electrode process. The relationship between the oxidation peak potential and $\ln \nu$ was also constructed and the regression equation can be expressed as E_{pa} (V) = 0.021 $\ln \nu$ (V/s) + 1.084 (R = 0.9954). As for an adsorption-controlled and irreversible electrode process, according to Laviron, E_{pa} is defined by the following equation [33]:

$$E_{pa} = E^o + (RT/\alpha nF)\ln(RTk^0/\alpha nF) + (RT/\alpha nF)\ln \nu \quad (1)$$

Thus, the value of αn can be easily calculated from the slope of $E_{pa} - \ln \nu$. In this work, the slope is of 0.021, therefore, the αn calculated to be 1.2. Generally, α is assumed to be 0.5 in totally irreversible electrode process [34,35]. So, the number of electron (n) transferred in the electrooxidation of guanosine is 2.4. According to the result obtained in Section 2.3 that the number of electrons and protons involved in the oxidation process of guanosine is equal. Therefore, the electrochemical oxidation of guanosine on graphene–chitosan/nano-Fe_3O_4/GCE is a two-electron and two-proton process.

According to the results obtained in Section 3.5, accumulation can effectively increase the electrochemical response of guanosine. Therefore, the influences of accumulation potential and time were investigated. With increasing accumulation time from 0 to 350 s, the oxidation peak current increased gradually, and then the slight increase was observed when further extending accumulation time. Therefore, 350 s was chosen as the optimized accumulation time. The accumulation potential was investigated in the range from 0 to 0.90 V with the interval of 0.10 V. The maximum current response was obtained at 0.60 V. Thus this potential was applied for guanosine determination.

3.5. Electrochemically effective surface area

The electrochemically effective surface areas (A) of the bare GCE and modified GCEs can be calculated by chronocoulometry based on the Anson equation of $Q = (2nFAcD^{1/2}t^{1/2})/\pi^{1/2}$ [36]. According to the slope of the plot of Q versus $t^{1/2}$ obtained in 1.0×10^{-4} mol L^{-1} $K_3[Fe(CN)_6]$ containing 1.0 mol L^{-1} KCl (the diffusion coefficient D of $K_3[Fe(CN)_6]$ is 7.6×10^{-6} cm^2 s^{-1} [37]), A can be determined. In this work, the slopes of the curves of $Q - t^{1/2}$ were 5.126, 10.25, 87.41 and 110.4 μC/s for GCE, nano-Fe_3O_4/GCE, graphene–chitosan/GCE and graphene–chitosan/nano-Fe_3O_4/GCE,

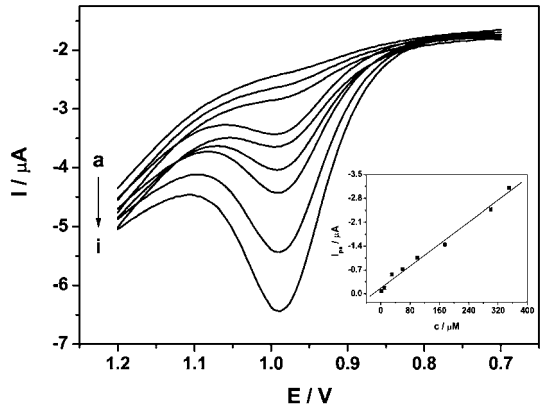

Fig. 7. Differential pulse voltammograms of graphene–chitosan/nano-Fe_3O_4/GCE in different concentrations of guanosine solutions. (a)–(i) 0, 2.0×10^{-6}, 1.0×10^{-5}, 3.0×10^{-5}, 6.0×10^{-5}, 1.0×10^{-4}, 1.75×10^{-4}, 3.0×10^{-4} and 3.5×10^{-4} mol L^{-1}. Insert: calibration curve.

respectively. Therefore, A was calculated to be 0.17, 0.34, 2.91 and 3.68 cm^2 for GCE, nano-Fe_3O_4/GCE, graphene–chitosan/GCE and graphene–chitosan/nano-Fe_3O_4/GCE, respectively. The results indicate that the electrode effective surface areas increased obviously after modification of GCE with graphene–chitosan and nano-Fe_3O_4, which will improve the adsorbance of guanosine, and then enhance the current response.

3.6. Calibration curve

Under the optimal conditions, differential pulse voltammetry (DPV) was used to determine guanosine due to its higher sensitivity than cyclic voltammetry. Fig. 7 shows the differential pulse voltammograms of different concentrations of guanosine in pH 7.0 PBS. As can be seen in the insert of Fig. 7, the oxidation peak current was proportional to guanosine concentration in the range of 2.0×10^{-6} to 3.5×10^{-4} mol L^{-1} with the linear regression equation of I_{pa} (10^{-6} A) = $-0.00807c$ (10^{-6} mol L^{-1}) $-$ 0.16764 (R = 0.9939). The detection limit was estimated to be 7.5×10^{-7} mol L^{-1} (S/N = 3). The calibration curves of guanosine at GCE, nano-Fe_3O_4/GCE and graphene–chitosan/GCE were also investigated. The linear ranges for GCE, nano-Fe_3O_4/GCE and graphene–chitosan/GCE were from 10 to 250 μM, 8 to 300 μM and 3.5 to 350 μM, respectively. The corresponding detection limits were 6.0, 4.5 and 0.95 μM (S/N = 3), which were higher than that at graphene–chitosan/nano-Fe_3O_4/GCE. The comparison of graphene–chitosan/nano-Fe_3O_4/GCE with other modified electrodes for guanosine determination was listed in Table 1. It can be seen that the graphene–chitosan/nano-Fe_3O_4/GCE offered reasonable linear range for guanosine detection and the detection limit was lower than some of previous reports. These results indicated that graphene–chitosan/nano-Fe_3O_4/GCE is an appropriate platform for the determination of guanosine.

3.7. Reproducibility, stability and interferences

For investigating the fabrication reproducibility, a 1.0×10^{-5} mol L^{-1} guanosine solution was measured by six modified electrodes prepared independently and the RSD of the peak current was 3.19%, revealing excellent reproducibility. After the electrode was stored for 15 days at 4 °C in humidity environment, it could retain 90.75% of its original response, suggesting acceptable storage stability. In addition, 200-fold concentration of Na^+, Ca^{2+}, Mg^{2+}, Fe^{3+}, Al^{3+}, Zn^{2+}, Ni^{2+}, Cu^{2+}, F^-, Cl^-, SO_4^{2-}, CO_3^{2-}, PO_4^{3-} and NO_3^-; 100-fold concentration of adenosine, uric acid, ascorbic acid, dopamine, cysteine, glycin, glutamic acid do not interfere with the oxidation signal of 1.0×10^{-5} mol L^{-1} guanosine (peak current change < 5%). These results indicated that graphene–chitosan/nano-Fe_3O_4/GCE has an excellent selectivity for guanosine, and it might be applied to determine guanosine in real samples.

3.8. Simultaneous detection

Fig. 8 shows the differential pulse voltammograms of different concentrations of guanosine at the graphene–chitosan/nano-Fe_3O_4/GCE in the presence of 5.0×10^{-5} mol L^{-1} guanine. The peak current of guanosine increased with increasing guanosine concentration, while the peak height of guanine kept almost unchanged. The linear relationship between the peak current and guanosine concentration can be expressed as I_{pa} (μA) = $-0.0092c$ (μM) + 0.000023 (R = 0.9973) in the range of 2.0×10^{-6} to 3.0×10^{-4} mol L^{-1} with the detection limit of 7.5×10^{-7} mol L^{-1} (S/N = 3). The peak-to-peak separation for guanosine and guanine was about 0.294 V, which was large enough for the simultaneous determination of guanine and guanosine. As can be seen in Fig. 9, the peak currents of guanosine and guanine increased gradually and linearly with the increase of the corresponding concentra-

Table 1
Comparison of different modified electrodes for guanosine determination.

Electrodes	Methods	pH	Potential (V)	Linear range (10^{-6} mol L^{-1})	Detection limit (10^{-6} mol L^{-1})	References
Graphene–chitosan/nano-Fe_3O_4/GCE	DPV	7.0	0.984	2–350	0.75	This work
BDD electrode	DPV	7.0	1.2		10	[9]
GCE	DPV[a]	4.5	1.05	–	3	[38]
CILE	CV	4.5	1.13	1–100	0.261	[32]
Fullerene–C_{60}/GCE	DPV	7.2	0.96	0.5–1000	0.145	[7]
Au/ITO electrode	DPV	7.2	0.601	0.1–10	0.098	[39]
MWCNTs–CILE	DPV	5.0	1.067	0.1–40	0.078	[8]

CILE: carbon ionic liquid electrode.
[a] DPV with ultrasonic irradiation.

Table 2
Determination of guanosine in human urine samples.

Samples	Added ($\times10^{-6}$ mol L^{-1})	Found ($\times10^{-6}$ mol L^{-1})	RSD (%)	Recovery (%)
1	10.00	10.12	3.57	101.2
2	20.00	19.15	3.92	95.75
3	40.00	39.01	4.61	97.53
4	80.00	83.54	4.68	104.43

Table 3
Determination of guanosine in *Pinellia ternate*, *Raidx astragali* and *Angelica sinensis*.

Samples	Determined ($\times 10^{-6}$ mol L^{-1})	Added ($\times 10^{-6}$ mol L^{-1})	Founded ($\times 10^{-6}$ mol L^{-1})	RSD (%)	Recovery (%)
Pinellia ternate	7.26	5.00	11.97	3.31	97.63
Raidx astragali	13.42	5.00	18.14	4.27	98.48
Angelica sinensis	8.41	5.00	13.73	4.12	102.39

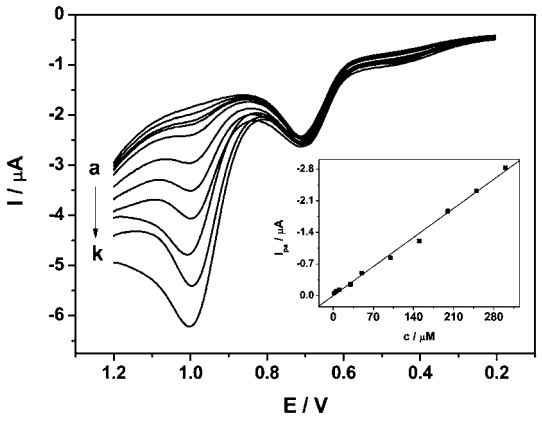

Fig. 8. Differential pulse voltammograms of guanosine at graphene–chitosan/nano-Fe_3O_4/GCE in 0.1 mol L^{-1} PBS (pH 7.0) with coexistence of 2.0×10^{-5} mol L^{-1} guanine. guanosine (a)–(k): 0, 2.0×10^{-6}, 5.0×10^{-6}, 1.0×10^{-5}, 3.0×10^{-5}, 5.0×10^{-5}, 1.0×10^{-4}, 1.5×10^{-4}, 2.0×10^{-4}, 2.5×10^{-4} and 3.0×10^{-4} mol L^{-1}. Insert: calibration curve.

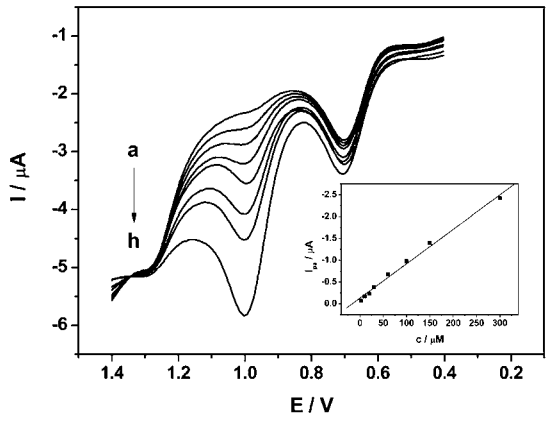

Fig. 10. Differential pulse voltammograms of guanosine at graphene–chitosan/nano-Fe_3O_4/GCE in 0.1 mol L^{-1} PBS (pH 7.0) with coexistence of 1.0×10^{-4} mol L^{-1} adenosine and 5.0×10^{-5} mol L^{-1} guanine. Guanosine (a)–(h): 2.0×10^{-6}, 1.0×10^{-54}, 2.0×10^{-5}, 3.0×10^{-5}, 6.0×10^{-5}, 1.0×10^{-4}, 1.5×10^{-4} and 3.0×10^{-4} mol L^{-1}.

tions in the range from 5.0×10^{-6} to 3.5×10^{-4} mol L^{-1}. Therefore, the fabricated electrode could be used to simultaneously determine guanosine and guanine. Additionally, the determination of guanosine was also carried out in the presence of guanine and adenosine with their concentration keeping constant (Fig. 10). The oxidation peak current of guanosine was proportional to its concentration in the range of 2.0×10^{-6} to 3.0×10^{-4} mol L^{-1}. Moreover, the peak-to-peak separation was 0.305 V for adenosine (1.29 V) and guanosine (0.985 V), and 0.294 V for guanosine and guanine (0.691 V), which were large enough for the performance of possible simultaneous determination of adenosine, adenosine and guanine.

3.9. Analytical application

In order to test the practical application of the proposed method, the graphene–chiotosan/nano-Fe_3O_4/GCE was used to determine guanosine in human urine samples. The urine samples were obtained from healthy volunteers, which were stored in plastic containers and used without dilution. No signals for guanosine were observed in these samples, which may be attributed to that no guanosine is in the human urine samples or the concentration of guanosine is lower than the detection limit. Therefore, the standard addition method was used. All the samples were determined for three times under the same conditions. The results were listed in Table 2. The recovery of guanosine was in the range from 95.75 to 104.43%, revealing that this method is effective, reliable and accurate. For further confirming the feasibility of the practical application, the fabricated electrode was used to determine guanosine content in *Pinellia ternate*, *Raidx astragali* and *Angelica sinensis*, which was purchased from a local drugstore. The determination results were shown in Table 3. The recovery was from 97.63 to 102.39%, which was acceptable.

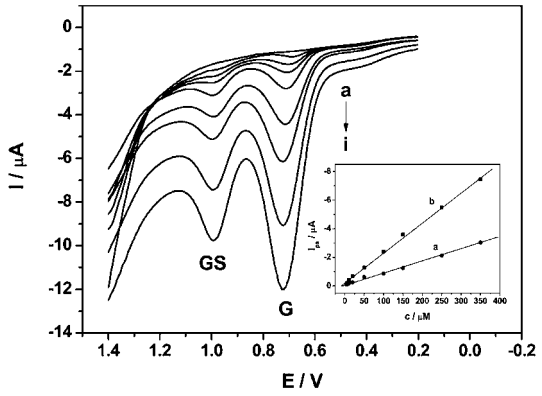

Fig. 9. Differential pulse voltammograms of guanosine at graphene–chitosan/nano-Fe_3O_4/GCE in 0.1 mol L^{-1} PBS (pH 7.0) with different concentrations of guanine. Guanosine and guanine (a)–(i): 0, 5.0×10^{-6}, 1.0×10^{-5}, 2.0×10^{-5}, 5.0×10^{-5}, 1.0×10^{-4}, $1.5.0 \times 10^{-4}$, $2.5.0 \times 10^{-4}$ and $3.5.0 \times 10^{-4}$ mol L^{-1}, respectively. Insert: calibration curve for guanine (b) and guanosine (a).

4. Conclusion

In this work, the electrochemical oxidation behavior of guanosine was investigated in details by the graphene–chitosan/nano-Fe_3O_4/GCE. Compared with GCE, chitosan/GCE, nano-Fe_3O_4/GCE and graphene–chitosan/GCE, the oxidation peak current increased obviously and the oxidation peak potential shifted more negatively on graphene–chitosan/nano-Fe_3O_4/GCE, indicating the excellent catalytic ability of the modified electrode. The proposed method can also be used to simultaneously determine guanosine, guanine and in the presence of adenosine. Under the optimal conditions, this new method was successfully applied to determine guanosine in spiked human urine and traditional Chinese medicine samples. Based on these, a new electrochemical method for guanosine determination was developed.

Acknowledgements

We are grateful to the financial support of the National Natural Science Foundation of China (No. 20775044) and the Natural Science Foundation of Shandong province, China (Y2006B20).

References

[1] M.E. dos Santos Frizzo, D.R. Lara, A.S. Prokopiuk, C.R. Vargas, C.G. Salbego, M. Wajner, D.O. Souza, Cell. Mol. Neurobiol. 22 (2002) 353.
[2] R. Ciccarelli, P. Ballerini, G. Sabatino, M.P. Rathbone, M. D'Onofrio, F. Caciagli, P. Di Iorio, Int. J. Dev. Neurosci. 19 (2001) 395.
[3] M.E. dos Santos Frizzo, F.A. Antunes Soares, L.P. Dall'Onder, D.R. Lara, R.A. Swanson, D.O. Souza, Brain Res. 972 (2003) 84.
[4] F. Caciagli, P. Di Iorio, P. Giuliani, P.J. Middlemiss, M.P. Rathbone, Drug Dev. Res. 50 (2000) 32.
[5] E. Regina Vinadé, A. Prato Schmidt, M. Em lio Santos Frizzo, I. Izquierdo, E. Elisabetsky, D. Onofre Souza, Brain Res. 977 (2003) 97.
[6] J. Yang, G. Xu, H. Kong, Y. Zheng, T. Pang, Q. Yang, J. Chromatogr. B 780 (2002) 27.
[7] R.N. Goyal, V.K. Gupta, M. Oyama, N. Bachheti, Talanta 71 (2007) 1110.
[8] W. Sun, Y. Li, Y. Duan, K. Jiao, Electrochim. Acta 54 (2009) 4105.
[9] E. Fortin, J. Chane-Tune, P. Mailley, S. Szunerits, B. Marcus, J.P. Petit, M. Mermoux, E. Vieil, Bioelectrochemistry 63 (2004) 303.
[10] S. Yang, D. Guo, L. Su, P. Yu, D. Li, J. Ye, L. Mao, Electrochem. Commun. 11 (2009) 1912.
[11] Y. Wang, Y. Li, L. Tang, J. Lu, J. Li, Electrochem. Commun. 11 (2009) 889.
[12] Y. Li, L. Tang, J. Li, Electrochem. Commun. 11 (2009) 846.
[13] C. Shan, H. Yang, D. Han, Q. Zhang, A. Ivaska, L. Niu, Biosens. Bioelectron. 25 (2009) 1070.
[14] C. Shan, H. Yang, J. Song, D. Han, A. Ivaska, L. Niu, Anal. Chem. 81 (2009) 2378.
[15] T.T. Baby, S.S.J. Aravind, T. Arockiadoss, R.B. Rakhi, S. Ramaprabhu, Sens. Actuators B 145 (2009) 71.
[16] J.-F. Wu, M.-Q. Xu, G.-C. Zhao, Electrochem. Commun. 12 (2009) 175.
[17] J. Lu, L.T. Drzal, R.M. Worden, I. Lee, Chem. Mater. 19 (2007) 6240.
[18] X. Kang, J. Wang, H. Wu, I.A. Aksay, J. Liu, Y. Lin, Biosens. Bioelectron. 25 (2009) 901.
[19] K. Zhou, Y. Zhu, X. Yang, J. Luo, C. Li, S. Luan, Electrochim. Acta 55 (2010) 3055.
[20] W.-J. Lin, C.-S. Liao, J.-H. Jhang, Y.-C. Tsai, Electrochem. Commun. 11 (2009) 2153.
[21] M. Zhou, Y. Zhai, S. Dong, Anal. Chem. 81 (2009) 5603.
[22] C. Shan, H. Yang, D. Han, Q. Zhang, A. Ivaska, L. Niu, Biosens. Bioelectron. 25 (2010) 1504.
[23] Y. Wang, Y. Wan, D. Zhang, Electrochem. Commun. 12 (2010) 187.
[24] H. Li, J. Chen, S. Han, W. Niu, X. Liu, G. Xu, Talanta 79 (2009) 165.
[25] D. Cao, N. Hu, Biophys. Chem. 121 (2006).
[26] Y. Cheng, Y. Liu, J. Huang, K. Li, Y. Xian, W. Zhang, L. Jin, Electrochim. Acta 54 (2009) 2588.
[27] D. Cao, N. Hu, Biophys. Chem. 121 (2006) 209.
[28] Y. Li, Y. Wu, J. Am. Chem. Soc. 131 (2009) 5851.
[29] S. Stankovich, D.A. Dikin, R.D. Piner, K.A. Kohlhaas, A. Kleinhammes, Y. Jia, Y. Wu, S.T. Nguyen, R.S. Ruoff, Carbon 45 (2007) 1558.
[30] Y. Lv, H. Wang, X. Wang, J. Bai, J. Cryst. Growth 311 (2009) 3445.
[31] R.N. Goyal, N. Jain, D.K. Garg, Bioelectrochem. Bioenerg. 43 (1997) 105.
[32] W. Sun, Y. Duan, Y. Li, H. Gao, K. Jiao, Talanta 78 (2009) 695.
[33] E. Laviron, J. Electroanal. Chem. 52 (1974) 355.
[34] K. Wu, Y. Sun, S. Hu, Sens. Actuators B 96 (2003) 658.
[35] F. Anson, Trans, in: W.Z. Huang (Ed.), Electrochemistry and Electroanalytical Chemistry, Peking University Press, Beijing, 1981.
[36] F. Anson, Anal. Chem. 36 (1964) 932.
[37] R. Adams, Electrochemistry at Solid Electrodes, Marcel Dekker, New York, 1969.
[38] A.M. Oliveira Brett, F.M. Matysik, Bioelectrochem. Bioenerg. 42 (1997) 111.
[39] R.N. Goyal, M. Oyama, A. Tyagi, Anal. Chim. Acta 581 (2007) 32.